Electronic Supplementary Material (ESI) for ChemComm.

"Superaerophobic" NiCo Bimetallic Phosphides for High-Efficient Hydrogen Evolution Reaction Electrocatalysts

*Ling Zhang[**a]; Jiawei Huang[**a]; Qizheng Zheng[a]; Ang Li[a]; Xianglan Li[a]; Jing Li[a]; Minhua Shao[b]; Hongmei Chen[a]; Zidong Wei[a]; Zihua Deng[*a], and Cunpu Li[*a]*

[a] The State Key Laboratory of Power Transmission Equipment & System Security and New Technology, Chongqing Key Laboratory of Chemical Process for Clean Energy and Resource Utilization, School of Chemistry and Chemical Engineering, Chongqing University, Shazhengjie 174, Chongqing 400044, China.

hg2531@cqu.edu.cn; zdwei@cqu.edu.cn

[b] Department of Chemical and Biological Engineering, Hong Kong University of Science and Technology, Clear Water Bay, Kowloon, Hong Kong, China. E-mail: kemshao@ust.hk

* To whom correspondence should be addressed.

** Ling Zhang and Jiawei Huang contributed equally.

Materials Synthesis

Materials: Nickel foam was purchased from Kunshan Kuangxun Ltd. (China). Pt/C (40% Pt on Vulcan XC-72R) was purchased from Sigma-Aldrich Chemical Reagent Co., Ltd., and 1,4-benzenedicarboxylic (BDC), KOH, Urea, $NiCl_2 \cdot 6H_2O$, $CoCl_2 \cdot 6H_2O$, $NaH_2PO_2 \cdot H_2O$, NH_4F from Shanghai Titan Science & Technology Co, Ltd. All reagents were used as received. The water used throughout all experiments was deionized water.

Synthesis of NiCo-MOF MPs: NiCo bimetal-organic framework (NiCo-MOF) were grown on nickel foam by a hydrothermal method (see Scheme 1). Take NiCo-MOF/Ni as an example. Firstly, 2.8 mmol of 1,4-benzenedicarboxylic (BDC) was dissolved in 35 ml water to form a turbid solution and then, the pH of the solution was kept at 8 by addition of 1 M NaOH with vigorous magnetic stirring for 15 min, referred to as Solution A. Secondly, 1.4 mmol of $CoCl_2 \cdot 6H_2O$, 1.4 mmol of $NiCl_2 \cdot 6H_2O$ and 8.4 mmol of NH_4F were dissolved in 35 ml water forming orange solution, referred to as Solution B. Subsequently, Solution A was mixed with Solution B under vigorous magnetic stirring until the solution turned transparent and yellow. The solution was then transferred into a 100 ml PTFE-lined stainless-steel autoclave containing a piece of clean nickel foam (1×5 cm^2). The autoclave was sealed and heated at 120 ^oC for 6 h. Afterwards, the autoclave was cooled to room temperature and then its content was taken out and washed with ethanol and water in turn before being dried at 60 ^oC in air for 12 h (denoted as NiCo-MOF MPs).

Preparation of NiCo-MOF-urea HPONs: 70 ml of 60 mM urea was added into a 100 ml PTFE-lined stainless-steel autoclave containing a piece of as-prepared NiCo-MOF MPs. The autoclave was sealed and heated at 140 ^oC for 6 h. After the autoclave was cooled to room temperature, its content (denoted as NiCo-MOF-urea HPONs) was taken out and washed with ethanol and water in turn before being dried at 60 ^oC in air for 12 h. Fixing other hydrothermal reaction conditions, the different samples were achieved by changing the reaction times to 3 h, 6 h, and 9 h and products denoted respectively as NiCo-MOF-urea-3 HPONs, NiCo-MOF-

urea-6 HPONs, and NiCo-MOF-urea-9 HPONs. For convenience, the NiCo-MOF-urea-60 HPONs also be denoted as NiCo-MOF-urea HPONs.

Preparation of Ni-Co-P HPONs: First, the NiCo-MOF-urea HPONs was calcinated in the air at 450 ^{o}C to obtain $NiCo_2O_4$ HPONs. And then, phosphidation of as-prepared $NiCo_2O_4$ HPONs was accomplished in a horizontal quartz tube furnace. Specifically, the NiCo-MOF-urea /Ni and $NaH_2PO_2{\cdot}H_2O$ were put individually in two porcelain boats. The boat with $NaH_2PO_2{\cdot}H_2O$ was placed at the upstream end of the furnace and the boat with $NiCo_2O_4$ HPONs at the other end. The molar ratio of metal to P was 1:10. The furnace was heated to 350 ^{o}C at a heating rate of 5 ^{o}C min^{-1} and maintained for 2 h in N_2 atmosphere (55 sccm). Then the reaction system was cooled naturally down to room temperature in the furnace to obtain final products Ni-Co-P.

Preparation of Ni-Co-P NSs: 2.8 mmol of $CoCl_2{\cdot}6H_2O$, 2.8 mmol of $NiCl_2{\cdot}6H_2O$, 5.6 mmol of NH_4F and 14 mmol of urea were dissolved in 70 ml water forming orange solution. The solution was then transferred into a 100 ml PTFE-lined stainless-steel autoclave containing a piece of clean nickel foam (1×5 cm^2). The autoclave was sealed and heated at 120 ^{o}C for 6 h. After the autoclave was cooled to room temperature, its content (denoted as NiCo-urea) was taken out and washed with ethanol and water in turn before being dried at 60 ^{o}C in air for 12 h. Phosphidation of as-prepared NiCo-urea was accomplished in a horizontal quartz tube furnace. Specifically, the NiCo-urea and $NaH_2PO_2{\cdot}H_2O$ were put individually in two porcelain boats. The boat with $NaH_2PO_2{\cdot}H_2O$ was placed at the upstream end of the furnace and the boat with NiCo-urea at the other end. The molar ratio of metal to P was 1:10. The furnace was heated to 350 ^{o}C at a heating rate of 5 ^{o}C min^{-1} and maintained for 2 h in N_2 atmosphere (55 sccm). Then the reaction system was cooled naturally down to room temperature in the furnace to obtain final products denoted as Ni-Co-P Nanosheet (Ni-Co-P NSs)

Structural Characterization

Powder X-ray diffraction (XRD) data were obtained using a PANalytical X'pert diffractometer with Cu Kα radiation (λ=1.5418 Å). The morphology and chemistry of the samples were characterized by a field emission scanning electron microscopy (FE-SEM) (model JSM-7800F, JEOL Ltd., Tokyo, Japan). Fourier transform infrared spectrometer (FTIR) is mainly used to describe the groups contained on the surface of catalytic materials and to study the structure and chemical bond of molecules. Transmission electron microscopy (TEM) measurements were performed on a HITACHI H-8100 electron microscopy (Hitachi, Tokyo, Japan) with an accelerating voltage of 200 kV. The energy dispersive X-ray (EDX) mapping was carried out to reveal the element composition and distribution in the samples. X-ray photoelectron spectroscopy (XPS) measurements were conducted by using a Thermo ESCALAB 250Xi with an Al Kα (1486.6 eV) X-ray source on the samples with binding energies referenced to adventitious carbon at 284.8 eV.

Electrochemical characterization

The electrocatalytic properties of the prepared samples were evaluated with Autolab (Auto 72703) electrochemical workstation in a conventional three-electrode system. Ni-Co-P hollow nanoprism, Ni-Co-P nanosheet and commercial Pt/C (40 wt% Pt/XC-72) on nickel foam were individually used as the working electrodes, a Hg/HgO electrode (1 M KOH) as the reference electrode, and a graphite plate as the counter electrode. The geometric surface area of the working electrode is 1.0×1.0 cm^2. The Hg/HgO reference electrode was calibrated with respect to RHE according to the previous study: in 1.0 M KOH saturated by H_2, $E_{RHE} = E_{Hg/HgO} + 0.0591*pH+0.098$. Prior to recording the hydrogen evolution activity, the catalysts were activated by 25 CV scans. Polarization curves were obtained using linear sweep voltammetry (LSV) conducted from 0.05 V to -0.7 V in 1.0 M KOH saturated by H_2 with a scan rate of 1 mV s^{-1}. The electrochemical impedance spectroscopy (EIS) was carried out at an overpotential of 100 mV in a frequency range from 100 kHz to 0.01 Hz. The polarization curves were corrected against ohmic potential drop.

Electrochemical active surface area

Cyclic voltammetry was used to measure the electrochemically active surface area (ECSA) in the non-Faraday range of 0.1- 0.2 V vs. RHE with different scan rates of 8, 11, 14, 17, 20, 23, 26, 29, 32 and 35 mV s^{-1}. Plotting the current density (j=(ja-jc)/2) at 0.15 V against the scan rate, the linear slope (= 166.5 mF) is the double layer capacitance (C_{dl}). The ECSA was calculated by dividing double-layer capacitance (C_{dl}) by the specific capacitance (Cs=40 μF cm^{-2}) of flat electrodes in 1 M KOH[1].

$$A_{ECSA} = \frac{C_{dl}}{C_S} = \frac{166.5mF}{40\mu F\ cm^{-2}} = 41625\ cm^{-2}$$

Bubble behavior study

The hydrogen bubbles behavior study on different electrodes were measured in 1 M KOH by Dataphysics Instruments OCA20, Germany. The diagram of measure the diffusion rates of H_2 on different electrodes are illustrated in Figure S1. The operation steps are present as follows:

(1) The Ni-Co-P HPONs (1cm x 1 cm) and the reference samples of Ni-Co-P NSs is immersed in 1 M KOH and fixed by a foam, which can keep the samples in the horizontal position.

(2) And them, H_2 gas (3 μL) is injected to their surface through a syringe needle.

(3) At last, open the digital video and photograph the bubble diffusion process.

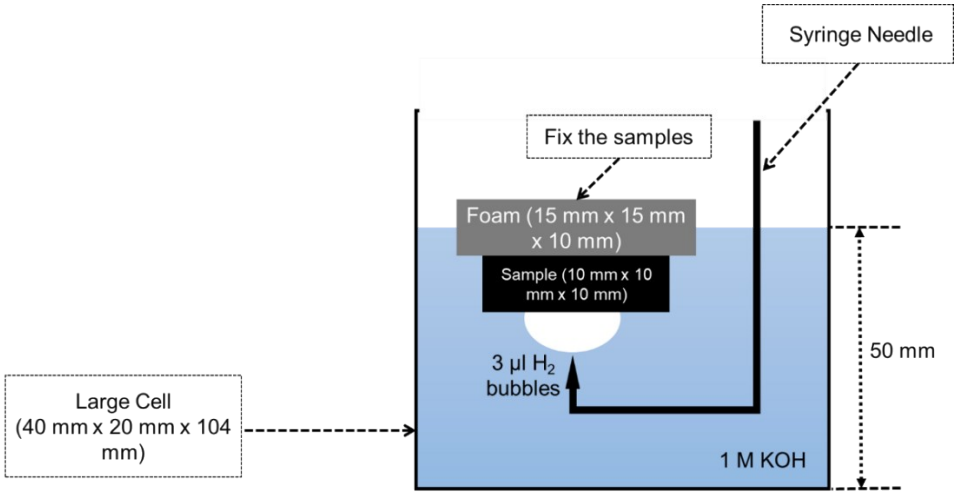

Figure S1 Diagram of measure the diffusion rates of H_2 on different electrodes

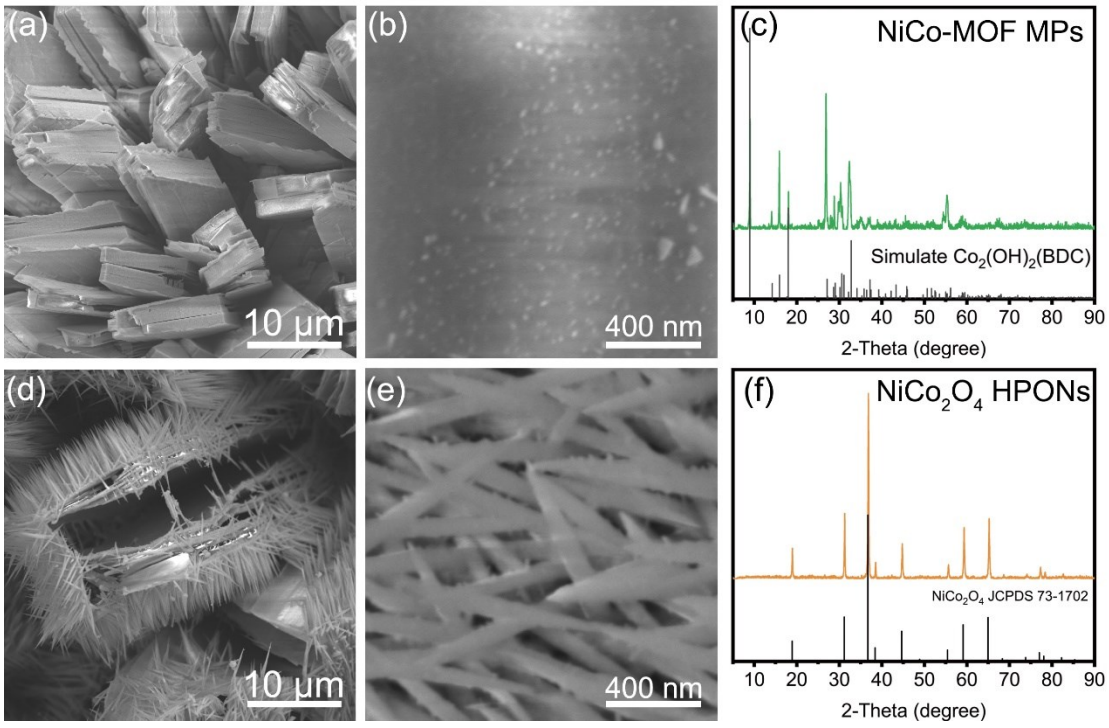

Figure S2 SEM images of NiCo-MOF MPs (a, b), and $NiCo_2O_4$ HPONs (d,e). XRD patterns of NiCo-MOF MPs (c), and $NiCo_2O_4$ HPONs (f).

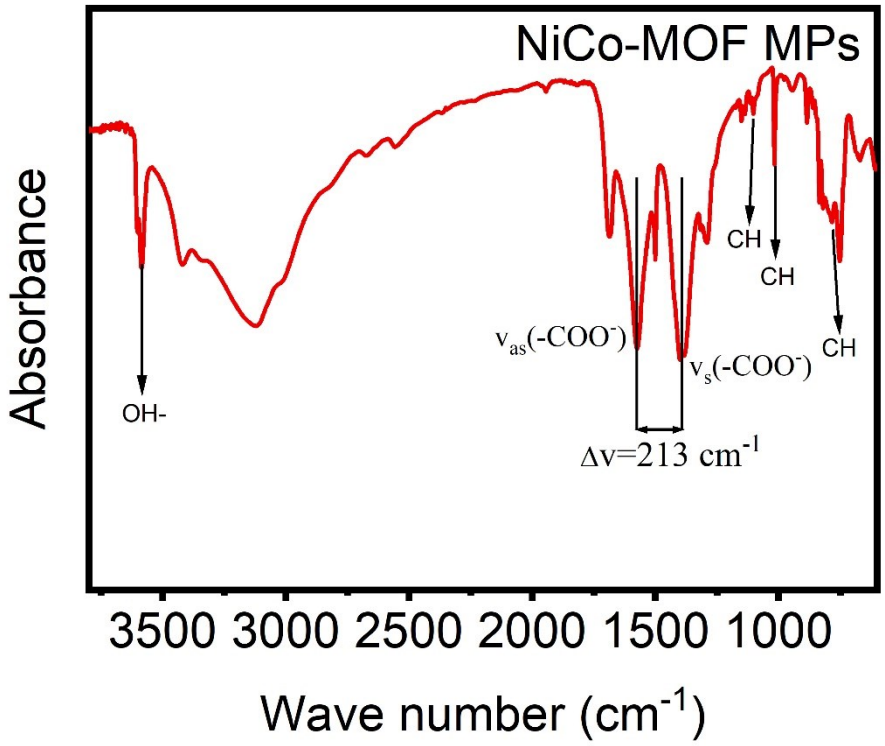

Figure S3 FTIR spectrum for NiCo-MOF MPs

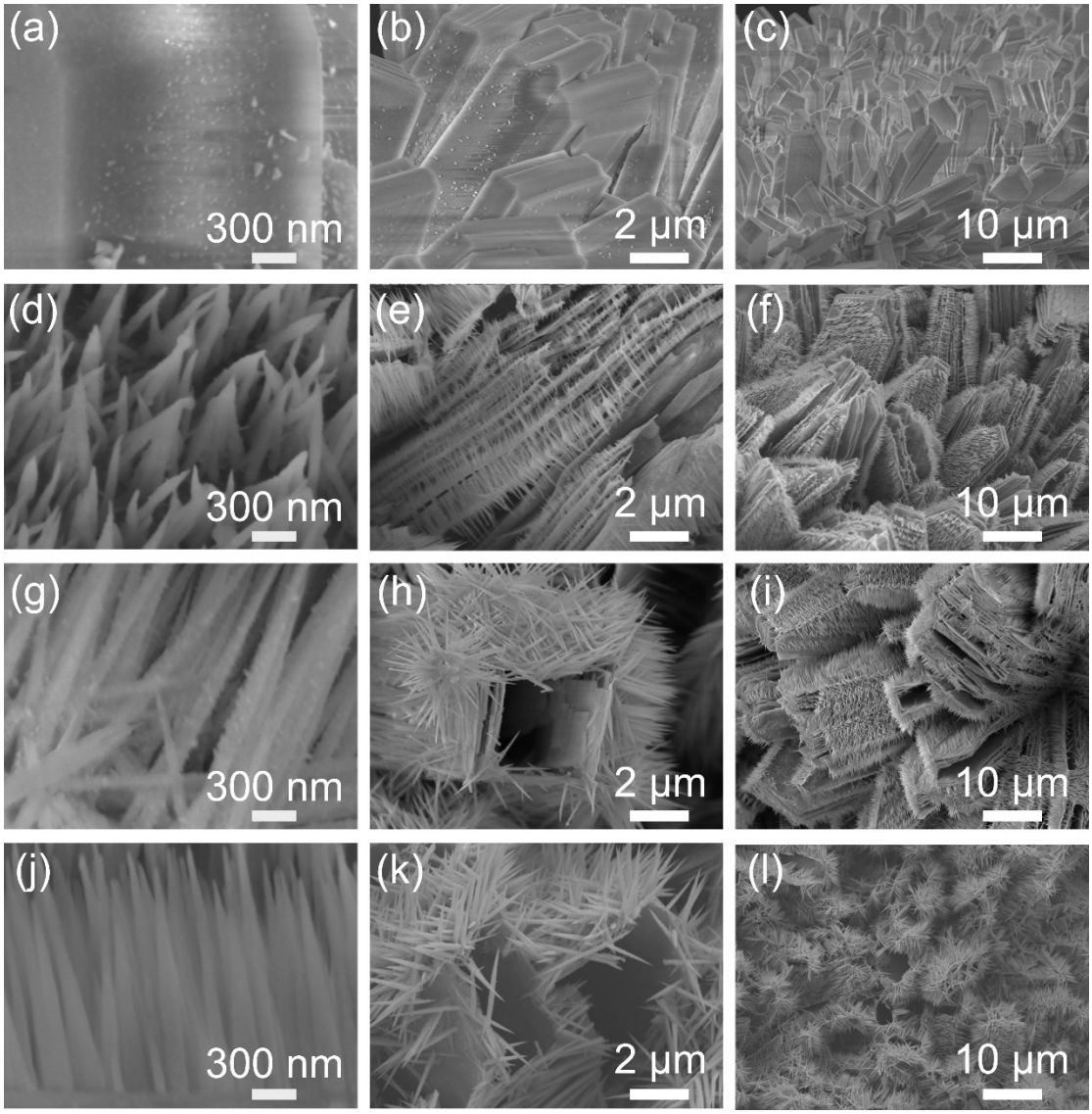

Figure S4 SEM images for NiCo-MOF MPs (a-c), NiCo-MOF-urea-3 HPONs (d-f), NiCo-MOF-urea-6 HPONs (g-i), and NiCo-MOF-urea-9 HPONs (j-l).

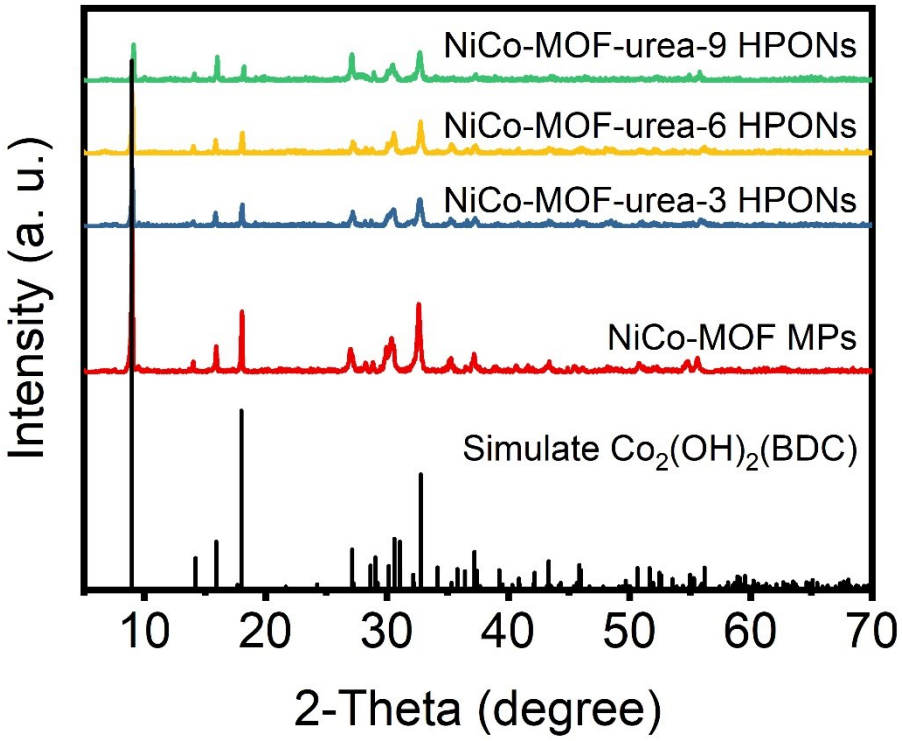

Figure S5 XRD patterns for NiCo-MOF MPs, and NiCo-MOF-urea-t HPONs (t = 3, 6, and 9).

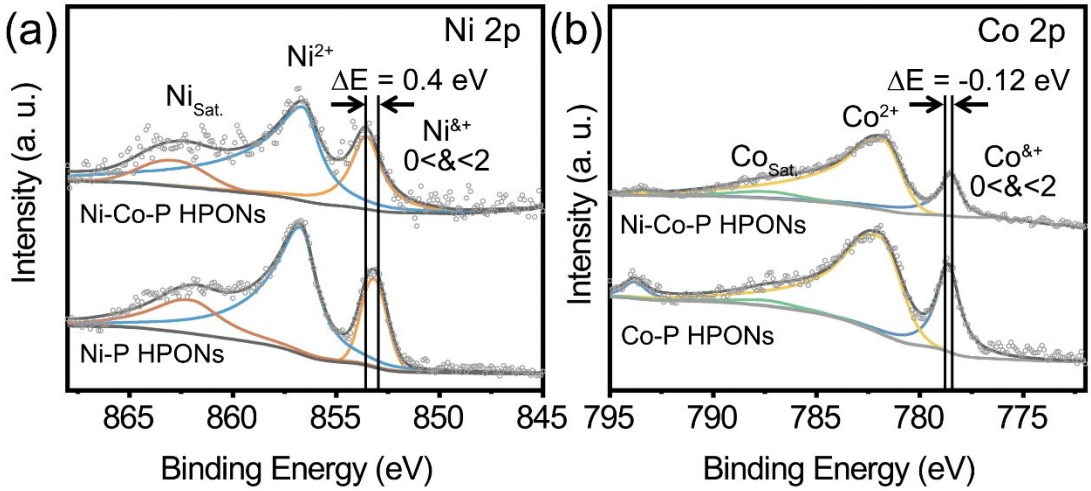

Figure S6 The Extended XPS spectrum for Ni-Co-P HPONs, Co-P HPONs, and Ni-P HPONs: (a) Ni 2p; (b) Co 2p.

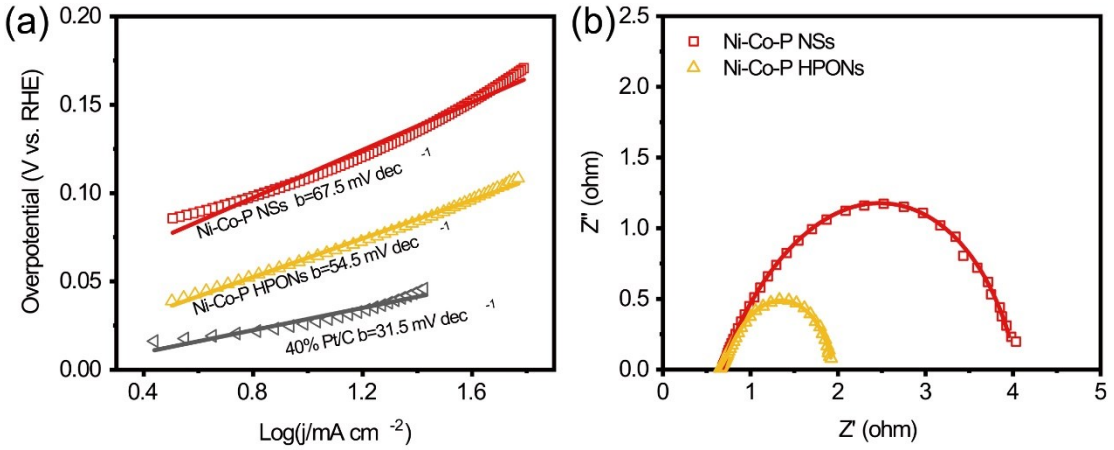

Figure S7 (a) Tafel plots curves of Ni-Co-P NSs, Ni-Co-P HPONs and the benchmark of 40% Pt/C. (b) EIS spectrum of Ni-Co-P NSs, Ni-Co-P HPONs.

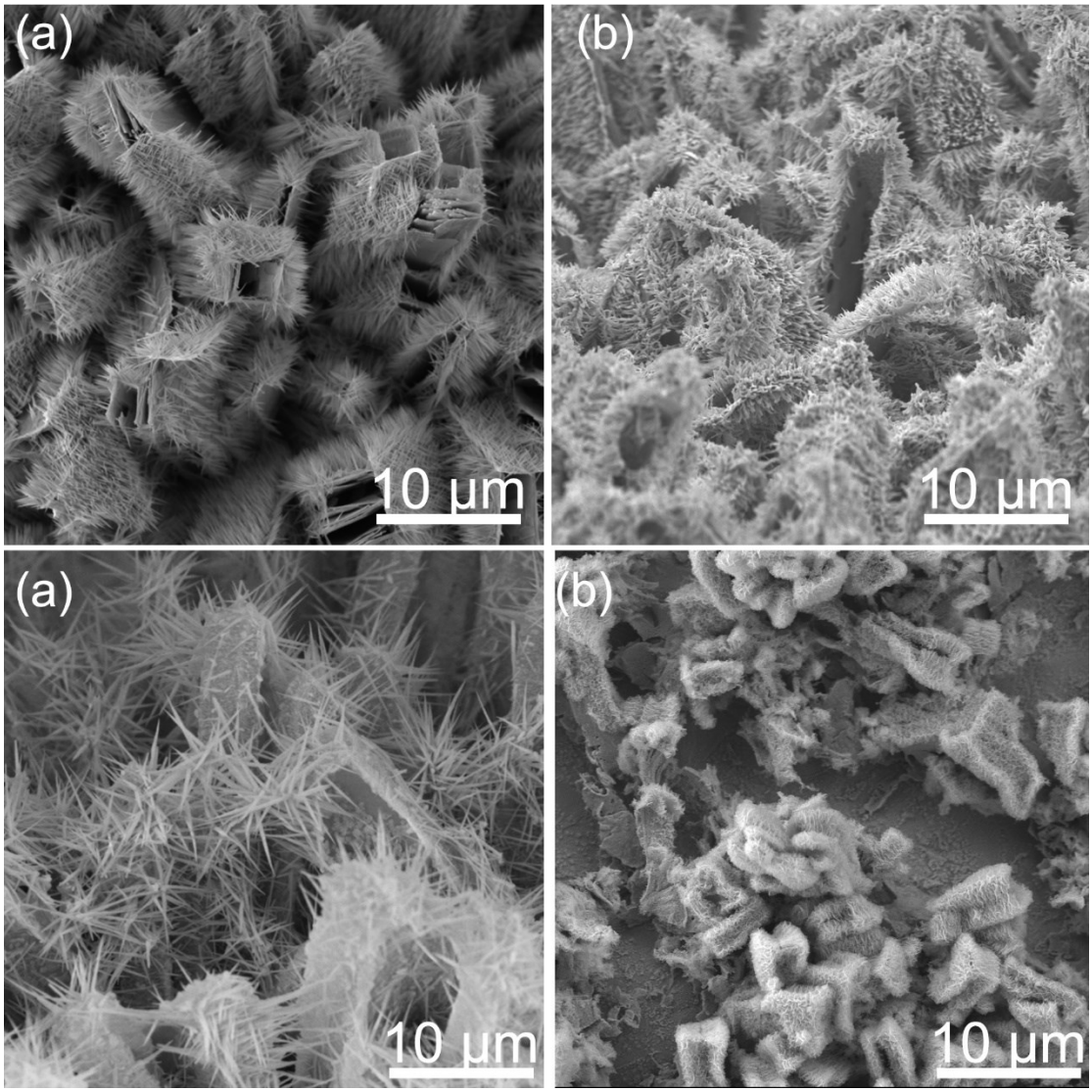

Figure S8 SEM images of Ni-Co-P HPONs before (a) and after stability test at current densities of -20 mA cm^{-2} (b), -100 mA cm^{-2} (c), and -800 mA cm^{-2}

Table S1 Summary of HER activities of Ni-Co-P NSs , Ni-Co-P HPONs and 40% Pt/C on the nickel foam.

Samples	$\eta_{10\ mA\ cm^{-2}}$ (mV)	$\eta_{500\ mA\ cm^{-2}}$ (mV)	$\eta_{800\ mA\ cm^{-2}}$ (mV)	Tafel Slope (mV dec^{-1})	$j_{0,\ geometric}$ (mA cm^{-2})	C_{dl} (mF cm^{-2})	Relative Surface Area
Ni-Co-P NSs	97	318	/	67.5	3.88	79.9	1
Ni-Co-P HPONs	27	173	205	54.5	4.55	166.5	2.09
40% Pt/C	19	/	/	31.5	4.58	/	/

Table S2 Comparison of HER performance of Ni-Co-P HPONs and other non-precious metal HER catalysts in 1 M KOH

Catalysis	η@10 mA cm^{-2} (mV)	Tafel slope (mV dec^{-1})	*Ref*
Ni-Co-P HPONs	27 mV@10 mA cm^{-2}	54.5	This work
	173 mV@500 mA cm^{-2}		
	205 mV@800 mA cm^{-2}		
CoP/CNT	67	54	2
Co_9S_8@NiCo LDH/NF	168	83	3
Co–Ni–P Film	103	49	4
CoP NW/Hb	78	62	5
CoP/Co_2P	68	40	6
Fe-CoP/Ti	75	78	7
FeCoP UNSAs	108	76	8
HS-Ni-Co-P	30	41	9
Ni-CoP/HPFs	92	71	10
CoP/Co-MOF	49	43	11
Co_4Ni_1P NTs	79	61	12
Ni_2P@NC	96	57	13
$Ni_{2-x}Co_xP$	50.7	42	14
Ni_5P_4	50	53	15
$Ni_{0.5}Co_{0.5}$ Nanowire	36	34	16
$NiCo/NiCo_2S_4$@NiCo Array	132	58	17
$NiCo_2P_x$	63	34.3	18
$NiCo_2O_4$	58	57	19
$Ni_{0.9}Co_{0.1}O_xH_y$	85	85	20
Ni–Co–MoS_2 Nanoboxes	125	52	21
Ni–Co–P Microflowers	117	69	22
Ni-Co-P Nanosheet	98	88	23
NiCoP-CoP/NF	73	91	24

Reference

1. H. Wang, C. Tsai, D. Kong, K. Chan, F. Abild-Pedersen, J. K. Nørskov and Y. Cui, *Nano Res.*, 2015, **8**, 566-575.
2. Q. Liu, J. Tian, W. Cui, P. Jiang, N. Cheng, A. M. Asiri and X. Sun, *Angew. Chem. Int. Edit.*, 2014, **53**, 6710-6714.
3. J. Yan, L. Chen and X. Liang, Sci. Bull., 2019, **64**, 158-165.
4. Y. Pei, Y. Yang, F. Zhang, P. Dong, R. Baines, Y. Ge, H. Chu, P. M. Ajayan, J. Shen and M. Ye, *ACS Appl. Mater Inter.*, 2017, **9**, 31887-31896.
5. J. Huang, Y. Li, Y. Xia, J. Zhu, Q. Yi, H. Wang, J. Xiong, Y. Sun and G. Zou, *Nano Res.*, 2017, **10**, 1010-1020.
6. Y. Hua, Q. Xu, Y. Hu, H. Jiang and C. Li, *J. Energy Chem.*, 2019, **37**, 1-6.
7. C. Tang, R. Zhang, W. Lu, L. He, X. Jiang, A. M. Asiri and X. Sun, *Adv. Mater.*, 2017, **29**.
8. L. Zhou, M. Shao, J. Li, S. Jiang, M. Wei and X. Duan, *Nano Energy*, 2017, **41**, 583-590.
9. P. Zhang, H. Chen, M. Wang, Y. Yang, J. Jiang, B. Zhang, L. Duan, Q. Daniel, F. Li and L. Sun, *J. Mater. Chem. A*, 2017, **5**, 7564-7570.
10. Y. Pan, K. Sun, Y. Lin, X. Cao, Y. Cheng, S. Liu, L. Zeng, W.-C. Cheong, D. Zhao, K. Wu, Z. Liu, Y. Liu, D. Wang, Q. Peng, C. Chen and Y. Li, *Nano Energy*, 2019, **56**, 411-419.
11. T. Liu, P. Li, N. Yao, G. Cheng, S. Chen, W. Luo and Y. Yin, *Angew. Chem. Int. Edit.*, 2019, **58**, 4679-4684.
12. L. Yan, L. Cao, P. Dai, X. Gu, D. Liu, L. Li, Y. Wang and X. Zhao, *Adv. Funct. Mater.*, 2017, **27**.
13. Z. Pu, C. Zhang, I. S. Amiinu, W. Li, L. Wu and S. Mu, *ACS Appl. Mater Inter.*, 2017, **9**, 16187-16193.
14. J. Li, M. Yan, X. Zhou, Z.-Q. Huang, Z. Xia, C.-R. Chang, Y. Ma and Y. Qu, *Adv. Funct. Mater.*, 2016, **26**, 6785-6796.
15. M. Ledendecker, S. Krick Calderon, C. Papp, H. P. Steinruck, M. Antonietti and

M. Shalom, *Angew. Chem. Int. Edit.*, 2015, **54**, 12361-12365.

16. P. Zou, J. Li, Y. Zhang, C. Liang, C. Yang and H. J. Fan, *Nano Energy*, 2018, **51**, 349-357.
17. Y. Ning, D. Ma, Y. Shen, F. Wang and X. Zhang, *Electrochim. Acta*, 2018, **265**, 19-31.
18. R. Zhang, X. Wang, S. Yu, T. Wen, X. Zhu, F. Yang, X. Sun, X. Wang and W. Hu, *Adv. Mater.*, 2017, **29**.
19. Z. Fang, L. Peng, Y. Qian, X. Zhang, Y. Xie, J. J. Cha and G. Yu, *J. Am. Chem. Soc.*, 2018, **140**, 5241-5247.
20. Q. Zhao, J. Yang, M. Liu, R. Wang, G. Zhang, H. Wang, H. Tang, C. Liu, Z. Mei, H. Chen and F. Pan, *ACS Catal.*, 2018, **8**, 5621-5629.
21. X. Y. Yu, Y. Feng, Y. Jeon, B. Guan, X. W. Lou and U. Paik, *Adv. Mater.*, 2016, **28**, 9006-9011.
22. X. Liu, S. Deng, D. Xiao, M. Gong, J. Liang, T. Zhao, T. Shen and D. Wang, *ACS Appl. Mater Inter.*, 2019, **11**, 42233-42242.
23. Y. Tian, J. Yu, H. Zhang, C. Wang, M. Zhang, Z. Lin and J. Wang, *Electrochim. Acta*, 2019, **300**, 217-224.
24. H. Liu, X. Ma, H. Hu, Y. Pan, W. Zhao, J. Liu, X. Zhao, J. Wang, Z. Yang, Q. Zhao, H. Ning and M. Wu, *ACS Appl. Mater Inter.*, 2019, **11**, 15528-15536.